Applied Mathematics & Information Sciences
An International Journal

http://dx.doi.org/10.12785/amis/080650

Algorithm of Shadow for Diffraction in Forests based on a Wireless Sensor Network

Yunjie Xu[1], *Wenbin Li*[1,*] *and Wei Zhang*[2]

[1] School of technology, Beijing Forestry University, Beijing, China
[2] School of technology, Zhejiang Agricultural & Forestry University, Linan, China

Received: 20 Nov. 2013, Revised: 18 Feb. 2014, Accepted: 19 Feb. 2014
Published online: 1 Nov. 2014

Abstract: Diffraction loss and the shadow of diffraction, which account for the growth of trees based on wireless sensors, long-distance, real-time, and accurate automatic acquisition of environmental information, were presented to meet the requirements for a wireless sensor network in a forest. Considering electromagnetic wave propagation, which accounts for the scattering and absorption behavior of plantations, a physical model of diffraction for a forest is constructed using the attenuation and the absorbing screens. The mathematical model of diffraction is presented using the uniform geometrical theory of diffraction. Moreover, the expression for diffraction loss is derived. The results were then applied to the birch. Simulation and analysis show the validity of the proposed model. The algorithm for diffraction loss can serve as a theoretical foundation for the optimization of the sensor layout and introduces a novel technology for the telemetry measurement of environmental information.

Keywords: Wireless sensor network, shadow of diffraction, man-made forest

1 Introduction

Wireless sensor network technology is extensively applied to industrial and agricultural production but is relatively less utilized in forestry production [1]. Numerous studies on the propagation loss of radio waves have been conducted, whereas studies on the propagation of high-frequency waves in forests are limited [2]. A complicated geographical environment results in severe signal attenuation [3,4,5]. ZigBee technology for wireless sensor networks was integrated into the survey of forestry resource information, and a new system was constructed based on this model. When power for this system is at 100 mill watts, communication distance is beyond 100 m in clearings and 50 m in forests, enabling the surveillance of a number of parameters, such as forestry biomass, temperature, and relative humidity, among others, which are then sent to a computer in a monitoring center. Continuous data acquisition on multi-standing trees, which are sampled from a forest and are less than 50 m away from one another, is achieved. Thus, the information transfer between sensors is fully implemented. The sensor has a data acquisition multi-interface connecting sensors for temperature, illumination, and soil moisture, among others, which are all placed at breast height, thereby achieving wireless communication through an organized meshwork between sensors. The system can practically be used in the dynamic monitoring of growing forest stock and in obtaining the biomass ranges of the trees growing in different directions. The information gathered using the proposed system is useful for policymaking on the prevention or control of forest fires [6,7] .

However, sensors were found to receive weak signals, or even none, when attached to a stem. This phenomenon is the diffraction of electromagnetic wave propagation. Diffraction occurs when electromagnetic waves are blocked by an obstacle, such as the edges of standing trees. A higher frequency results in a decrease in diffraction capability. The diffraction capability of a signal emitted by a 2.4 GHz sensor is not ideal because of the anti-jamming of electromagnetic and instability. Thus, the shadow of signal occurs at the rear of the standing tree. If the field and region of the shadow are accurately determined, the sensor can be installed correctly, enabling effective communication [8].

Results show that signal frequency, stem form, and propagation direction, among others, affect the diffraction fields and the shadow of diffraction. In the current paper, the algorithm of the diffraction fields in a forest is

* Corresponding author e-mail: leewb@bjfu.edu.cn

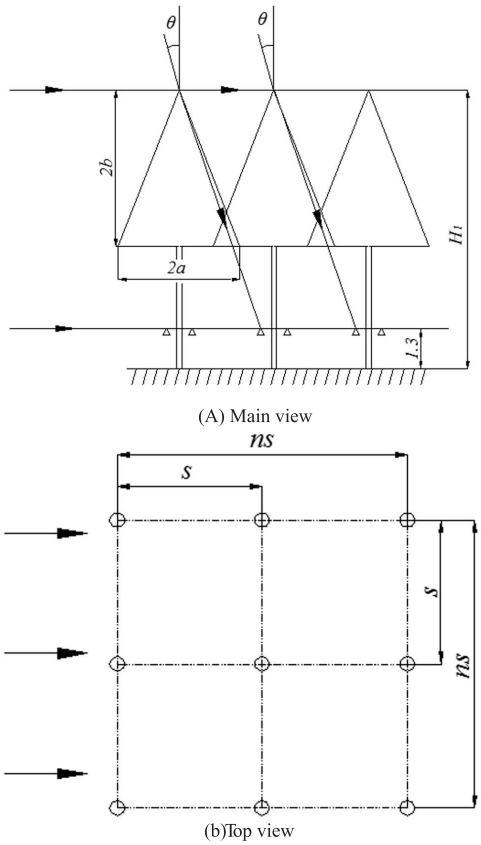

Fig. 1: Signal transmission model of plantation

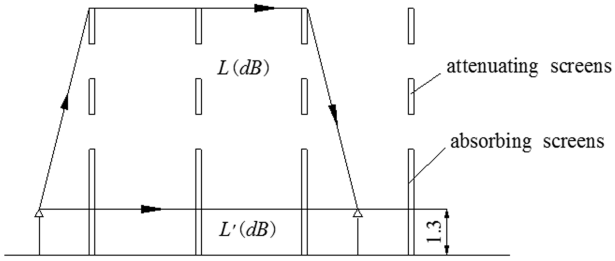

Fig. 2: Radio propagation loss model

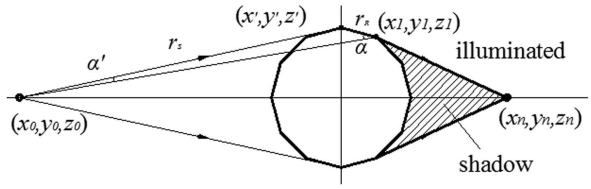

Fig. 3: Simplified polygon model of standing trees

presented by the application of the electromagnetic wave propagation and experimentation.

2 Physical model of diffraction for plantation

The distinction between natural and plantation forests has become clearer because of the intensive management in terms of the planting of single species, uniform planting densities, age classes, and shorter rotation. To gain insight on the significant effects of trees, an ideal diagram of continuous rows of planted trees is shown in Fig. 1.

Tree trunks are replaced by absorbing screens. The leaves and branches are replaced by partially attenuate screens. The phase and attenuation screen are located directly above the absorbing screen for simplicity. The propagation loss model is shown in Fig. 2.

The wireless sensor placed at a breast height of 1.3 m can be further lowered to the basal area in the current paper [9], thus only the effects of the basal area of breast height are considered. Circular area expressions are used for the measurements of the basal area of breast height and standing wood volume, with an average error of $\pm$ 3% [9].

The diffraction fields and the shadow of standing tree diffraction are solved using polygons as approximate substitutes for the circle. The model is shown in Fig. 3, where (x_0, y_0, z_0) is the source point, (x', y', z') is the secondary source point, and (x_1, y_1, z_1) and (x_n, y_n, z_n) are the receiver points with the number border of polygon n, which is determined by the breed and diameter of the tree. The radial can be divided into two components. The first component is the incident energy propagates straightly based on the law of geometrical optics, and the second is the incident energy propagates along the edge of a standing tree, and the shadow and transition regions are formed when the radial of the edge continuously emits diffracted radials along the tangency. Based on the uniform geometrical theory of diffraction (UTD), the region of transition is uniform. To account for the disposal of the sensor, only the illuminated region and the shadow are considered in the current paper.

3 The mathematical model of diffraction for plantation

To model the propagation, Tamir represents the forest using a lossy dielectric layer with a complex dielectric constant at ultra high frequency (UHF) (200–2000 MHz). Tamir's model no longer holds because only the absorption of plantations is considered, and the scattering behavior of scatters (tree trunks, leaves, and branches) is excluded.

Thus, the plantation is considered as discrete random-medium that can be represented as a time-invariant ensemble of randomly positioned and oriented canonical

scatterers. The electromagnetic wave propagation in this medium may be represented as the sum of two components, namely, attenuation screen loss of diffraction $L(dB)$ and absorbing screen loss $L'(dB)$.

3.1 Attenuation screen loss of diffraction

At UHF, the principal mechanism responsible for long-distance propagation is the lateral wave, which skims along the tree tops. The average field of attenuation screen is given by the following equation [4]:

$$E(x,z,q) = q_x \exp[jkx - jk_0 \cos(\theta_i)z] \tag{1}$$

where
$k = k_0 \sin(\theta_i) + \frac{2\pi}{k_0 \sin(\theta_i)} \sum_t \rho_t (f_{|x|}^{(t)}(i,i))$, $f_{|x|}^{(t)} = pf(o,i,q)$, k is the wave propagation constant along the x direction$t$ is the type of scatteringand ρ_t is the density of scatterers. $f_{|x|}^{(t)}(i,i)$ is the amplitude of the average forward scattering as follows:

$$f_{|x|}^{(t)}(i,i) = \int f_{|x|}^{(t)}(i,i) p(\theta) d\theta \tag{2}$$

$p(\theta)$ is probability density function of the scattering angle.

The crown is a lossy dielectric layer, so k of the wave propagation constant is complex in the crown, that is, $k = \beta + jL(dB)$. $L(dB)$ is the attenuation constant of the wave propagation, with the loss model of wave propagation as follows:

$$L(dB) = 8.686 \mathrm{Im}\left[k_0 \sin(\theta_i) + \frac{2\pi}{k_0 \sin(\theta_i)} \sum_t \rho_t f_{|x|}^t(i,i)\right] (dB/m) \tag{3}$$

3.2 Absorbing screen loss

When shadowing results from a single object, such as a standing tree, the attenuation attributable to diffraction can be estimated by considering the obstruction a diffracting wedge-edge.

To describe the diffraction effects of the edges of surfaces using a relatively simple mathematical method, the Kirchhoff–Huygens approximation is employed [10]. According to the Kirchhoff approximation, the receiver point(x_1, y_1, z_1) can be written as an integral for the complex amplitude over the plane $x = 0$, reference [11] given by the following equation:

$$E(x_1,y_1,z_1) \approx \int_{-\infty}^{+\infty} \int_{-\infty}^{+\infty} (\cos\alpha + \cos\alpha') E^{inc}(0,y',z') \frac{jke^{-jkr_R}}{4\pi r_R} d_{y'} d_{z'} \tag{4}$$

where r_R is the distance from the secondary source point in the plane $x = 0$ to the receiver point (x', y', z'), and $E^{inc} = A_0 e^{-jkx}$ is the amplitude of the secondary source.

$r_s \gg r_R$, so the distance from the source to the y axis is significantly greater than that of the receiving point to the y axis. Thus, the wave generated by the source is approximately considered as the plane wave entering from the left to the fringe, with $x = 0$ standing trees. Considering the uneven surface of trees, the fringe of a standing tree is simplified as an absorbing screen. If the plane wave propagates along the x axis and $r_s \gg r_R$, then the incident angle is $\alpha' = 0$. The model can be further simplified, as shown in Fig. 4, where α' is the diffraction angle, and the wedge angle $\beta = (2-n)\pi (1 < n < 2)$. The location of angle α below the x axis is the shadow boundary, and the shadow region below the boundary exists only as the diffraction field.

Without loss of generality, the receiver points are assumed to lie in the plane $Z = 0$ because of the translation symmetry along Z (trunk height direction). With the foregoing assumptions, the diffracted field through the edge for standing tree is given as follows:

$$E(x_1,y_1,0) = A0 \frac{jk}{4\pi} \int_0^{+\infty} \int_{-\infty}^{+\infty} (1+\cos\alpha) \frac{e^{-jkr_R}}{r} {}_R d_{z'} d_{y'} \tag{5}$$

where the distance from the integration point to the receiver point $r_R = \sqrt{x_1^2 + (y_1 - y')^2 + (z')^2}$.

To perform the z' integration in Eq. (5), the primary contribution to the integral comes from a region of z' that is given by the Fresnel zone, which is small compared with x, i.e., $x \gg \lambda$. The center of this region is the stationary-phase point, where the derivative of the exponent k_{rR} with respect to z vanishes. r_R in the denominator and $\cos\alpha$ will hardly vary and can be treated as constants.

r_R can be expanded to the second order according to ρ_R, with $\rho_R = \sqrt{x_1^2 + (y_1 - y')^2}$, and thus, $r_R = \rho_R + (z')^2 / 2\rho_R$.

Substituting r_R into Eq. (5), the integration over z' is reduced as follows:

$$\begin{aligned} E(x_1,y_1,0) =& A_0 \frac{jk}{4\pi} \int_0^{+\infty} \int_{-\infty}^{+\infty} (1+\cos\alpha) \frac{e^{-jkr_R}}{r_R} d_{z'} d_{y'} \\ E(x_1,y_1,0) \approx& A_0 \frac{jk}{4\pi} \int_0^{+\infty} (1+\cos\alpha) \frac{e^{-jk\rho_R}}{\rho_R} \\ & \left[\int_{-\infty}^{+\infty} \exp\left[-jk\frac{(z')^2}{2\rho_R}\right] dz'\right] \end{aligned} \tag{6}$$

Using the substitution $u = z' e^{j\pi/4} \sqrt{k/2\rho_R}$ to perform integral transform, Eq. (5) changes into the following:

$$\begin{aligned} E(x_1,y_1,0) \approx& A_0 \frac{jk}{4\pi} \int_0^{+\infty} (1+\cos\alpha) \frac{e^{-jk\rho_R}}{\rho_R} e^{j\pi/4} \sqrt{\frac{2\pi\rho_R}{k}} dy' \\ =& A_0 \frac{e^{j\pi/4}}{2} \sqrt{\frac{k}{2\pi}} \int_0^{+\infty} (1+\cos\alpha) \frac{e^{-jk\rho_R}}{\sqrt{\rho_R}} dy' \end{aligned} \tag{7}$$

Similarly, the expression $\rho_R = \sqrt{x_1^2 + (y_1 - y')^2}$ can be expanded to the second order as $\rho_R = \rho - y' \frac{y_1}{\rho}$ according

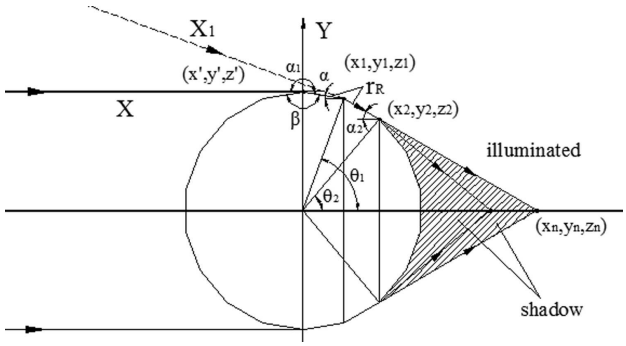

Fig. 4: The simplified model of wedge diffraction

to ρ, with $\rho = \sqrt{x_1^2 + y_1^2}$. θ_1 is the angle between the x axis and the line from the edge to the receiver point, and thus, $\sin\theta_1 = y_1\rho$.

Using the substitution $v = y'e^{-j\pi/4}\sqrt{k/\rho}$ to perform integral transform, Eq. (**??**) turns into the following:

$$\begin{aligned} E(x_1,y_1,0) &= A_0\frac{e^{j\pi/4}}{2}\sqrt{\frac{k}{2\pi}}\left[\int_0^{+\infty}(1+\cos\alpha)\frac{e^{-jk\rho_R}}{\sqrt{\rho_R}}dy'\right] \\ &\approx A_0\frac{e^{j\pi/4}}{2}\sqrt{\frac{k}{2\pi}}(1+\cos\theta)\frac{e^{-jk\rho}}{\sqrt{\rho}}\int_0^{+\infty}\exp\left(jky'\frac{y}{\rho}\right)dy' \\ &= A_0e^{-jk\rho}\bullet\left(-\frac{e^{j\pi/4}}{\sqrt{2\pi k\rho}}\frac{1+\cos\theta}{2\sin\theta}\right) \end{aligned} \tag{8}$$

When performing the integration in Eq. (8), k is given a vanishingly small negative imaginary part, as appropriate for atmospheric absorption, to ensure convergence at the lower limit. However, after the integration, k can be taken to be real. When the diffraction coefficient $D(\theta_1) = -e^{j\pi/4}(1+\cos\theta_1)/(2\sin\theta_1\sqrt{2\pi k\rho})$, and when $E^{inc} = A_0e^{-jkx}$ is substituted into Eq. (8), the following is derived:

$$E(x_1,y_1,0) = A_0e^{-jk\rho}D(\theta_1) = E^{inc}(0,y',z')e^{-jk\rho}D(\theta_1) \tag{9}$$

Similarly, (x_1, y_1, z_1) is the secondary source point and (x_2, y_2, z_2) is the receiver point obtained using the following simplified procedure:

$$\begin{aligned} E(x_2,y_2,0) &= E^{inc}(x_1,y_1,0)e^{-jk\rho}\bullet\left(-\frac{e^{j\pi/4}}{\sqrt{2\pi k\rho}}\frac{1+\cos\theta_2}{2\sin\theta_2}\right) \\ &= E^{inc}(x_1,y_1,0)D(\theta_2)e^{-jk\rho} \end{aligned} \tag{10}$$

In this equation, θ_2 is the angle between the X_1 axis and the line from the edge to the receiver point, and thus, $\sin\theta_2 = y_2/\rho$, where the diffraction coefficient is as follows:

$$D(\theta_2) = -\frac{e^{j\pi/4}}{\sqrt{2\pi k\rho}}\frac{1+\cos\theta_2}{2\sin\theta_2}$$

Accounting for the influence of the diffusion factor $A(s)$ and according to UDT, the aforementioned approach can also be used to derive the field at the receiver point of (x_n, y_n, z_n) as follows:

$$E^n(s) = E^{n-1}(Q)D(\theta_n)A(s)\exp(-jks) \tag{11}$$

where $E^n(s)$ represents the diffraction field of the location s distance from the diffraction point Q, $E^n(Q)$ represents the incident end-field of the radial at the diffraction point Q, $D(\theta_n)$ is the diffraction coefficient, the diffusion factor is $A(s) = 1/\sqrt{s}$, $\exp(-jks)$ is the phase delay factor, and the wave number is $k = 2\pi/\lambda$.

Suppose E_i is the incident field. From Eq. (9), the diffraction field E_d of the receiver satisfies $E^n(s) = E^{n-1}(Q)\ D(\theta_n)A(s)exp(-jks)$. Then, considering an incident plane wave, the diffraction loss of the receiver power can be written in the following form:

$$L(dB)' = 20\log\left(\frac{E_d}{E_i}\right)(dB) \tag{12}$$

Therefore, the electromagnetic wave propagation is represented as the sum of two components:

$$L = L(dB) + L(dB)' \tag{13}$$

4 Model simulation result and analysis

Taking man-made birch as example, the frequency of the source point in the base station is $f = 2.4$ GHz, the circumference of the standing tree is $l = 1.1$ m, the radius of standing tree is $a = l/2\pi$, and source and receiver are equal in height, that is, diameter at breast height $z =$ 1.3 m. The distance of the secondary source point located at (x, y', z') along the negative Y axis is $y' =$ a, and the location of the receiving point located at (x', y', z') along the positive Y- axis is $y_1 = a \times \sin\theta$. The wedge angle is $\beta = 150^\circ$, the relative dielectric constant is $\varepsilon_r = 2.727$, and the conductivity is $\sigma \approx 0$.

The variation between the diffraction loss and the dodecagon angle (Wedge angle) is shown in Fig. 5. The variation between the diffraction loss and frequency of source is shown in Fig. 6.

Fig. 5 shows the inverse relationship between the diffraction loss of the receiver power and the wedge angle. The diffraction loss of the receiver power rapidly decreases with increasing wedge. When the wedge angle is $\beta > 150^\circ$, the receiving antennae in the deep region of diffraction is near the wedge plant. Figure 6 shows that the propagation loss of the receiver power increases with an increase in the distance of the source, i.e., if the propagation loss increases, the free space propagation loss also increases.

From Fig. 7, we can see good consistency between the measured value and simulated value, which indicates that in 2.4 GHz frequency, the ray tracing method is able to

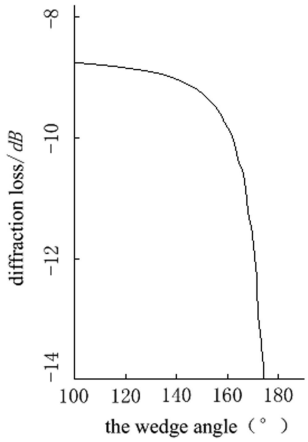

Fig. 5: Variation between diffraction loss and the wedge angle

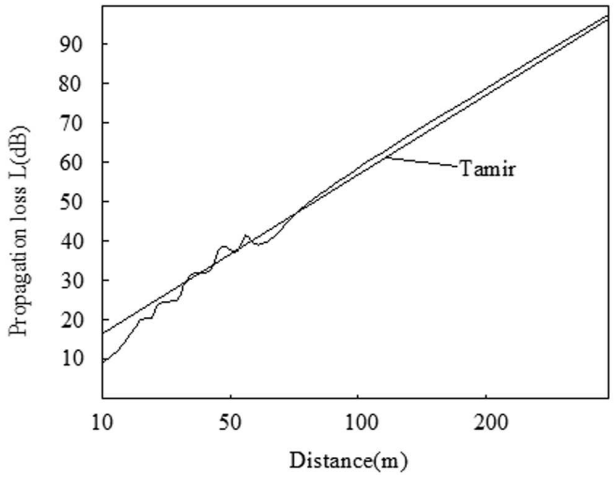

Fig. 6: The variation between propagation loss and distance

effectively predict the path loss characteristics in the planted forest environment. Furthermore, the predicted values of path loss on the test point are generally smaller than the measured values, which is caused by the simplification of planted forest environment and living woods during simulation as well as the error of propagation model. For example, the simulated value neglects the impact of secondary or multiple diffraction and reflection.

5 Conclusion

In conclusion, the layout of sensors for environmental information and the problem of diffraction loss and the shadow of diffraction in optimization are discussed. The physical model of diffraction on plantation is presented using the principle of Fresnel–Kirchhoff and the UTD. Moreover, the expression and capability for diffraction

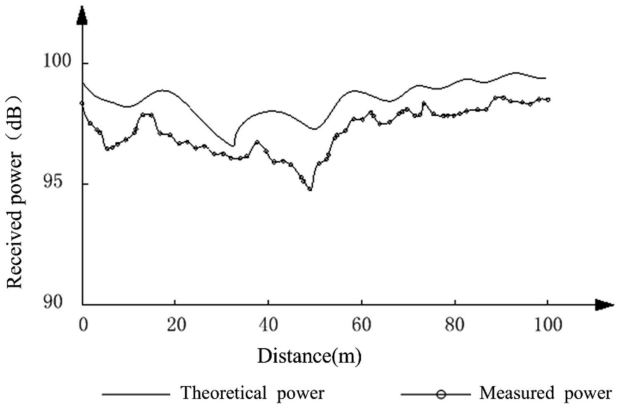

Fig. 7: Comparison of theoretical power and measured power

loss are analyzed, and the algorithm of the shadow is briefly discussed. Finally, the feasibility and validity of the UTD for computing the diffraction loss of plantation is verified using theoretical analysis and simulation. This approach can compute, analyze, and evaluate the diffraction loss field and shadow. The algorithm of diffraction can serve as a theoretical foundation for the optimization of the layout of sensors and introduces a novel technology for the telemetry measurement of environmental information.

Acknowledgements

This work was supported in part by the National Natural Science Foundation of China (Grant No. 30972425) and the Natural Science Foundation of Zhejiang Province of China (Grant No. LY12C16003). Supported by Scientific Research Foundation, Zhejiang Agricultural & Forestry University of China (Grant No. 2012FR101). Public Interest Research agricultural projects of Zhejiang Province of China (Grant No.2011C22021).

References

[1] Q.P. Wang, H.W. Li, Z.J. Qi, Journal of Agricultural Mechanization Research, **5**, 209-211 (2005).
[2] T. Fukatsu, M. Hirafuji, Journal of Robotics and Mechatronics, **17**, 164-172 (2005).
[3] K.Q. Hu, Z.T. Fu, R.H. Ji, L.J. Qi, Sensor Letters, **9**, 1220-1224 (2011).
[4] W.B. Li, J.M. Zhang, C. Sa, D.M. Wang, K. Gao, Journal of Beijing Forestry University, **29**, 15-18 (2007).
[5] Z.Y. Jiang, P.N. Jiao, Journal of China Institute of Communications, **13**, 73-78 (1992).
[6] J.G. Zhang, W.B. Li, N. Han, J.M. Kan, Journal of Beijing Forestry University, **29**, 41-45 (2007).
[7] J.G. Zhang, W.B. Li, Y.D. Zhao, Computer Engineering & Science, **35**, 62-64 (2008).

[8] S.Q. Han, Y. Zhang, Sensor Letters, **9**, 1485-1489 (2011).
[9] Y.M. Xian, Forest mensuration, China Forest Press, (1995).
[10] B.B. Baker, E.T. Copson, The Mathematical Theory of Huygens Principle, Qxford University Press, London, (1953).
[11] J.H. Whltteker, Radio Sci., **25**, 837-851 (1990).
[12] B.G. Lee, Y.C. Wan, Sensor Letters, **9**, 234-242 (2011).
[13] Y.J. Xu, W.B. Li, Second International Conference on Future Computer and Communication, **3** 251-254 (2010).
[14] Y.J. Xu, W.B. Li, Advanced Science Letters, **6**, 558-562 (2012).
[15] Y.J. Xu, W.B. Li, International Journal of Advancements in Computing Technology, **4**, 315-323 (2012).

Yun-jie Xu received B.S., M.S. and Ph.D. degrees in forest engineering from the University of Beijing Forestry of China, Beijing, China, in 1998, 2004, and 2012, respectively. From April 2004 to Dec. 2010, he was a faculty with the School of technology , Zhejiang Agricultural & Forestry University and was promoted to be an associate professor in 2011. His current research interests include system fault diagnosis and signal propagation in forest.

Wen-bin Li received M.S. and Ph.D. degrees in Shizuoka University and Ehime University, Japan, in 1987, and 1990, respectively, Ph.D. advisor. From 1992 to Dec. 2012, he was a faculty with the School of technology, Beijing Forestry University and was promoted to be a professor in 1996. His current research interests include forestry Forestry machinery automation and intelligent.

Wei Zhang received B.S., M.S. and Ph.D. degrees in forest engineering from Zhejiang University of Technology and the University of Beijing Forestry of China, Beijing, China, in 1992, 2005, and 2009, respectively. From April 2002 to Dec. 2012, he was a faculty with the School of technology , Zhejiang Agricultural & Forestry University and was promoted to be an associate professor in 2006. His current research interests include system fault diagnosis and signal propagation in forest.